

## The Magnetic and Crystallographic Properties of MnBi Studied by Neutron Diffraction

A. F. ANDRESEN

*Institutt for Atomenergi, Kjeller, Norway, and Delegation AF, Eidgenössisches Institut für Reaktorforschung, Würenlingen, Switzerland*

W. HALG, P. FISCHER and E. STOLL

*Delegation AF, Eidgenössisches Institut für Reaktorforschung, Würenlingen, Switzerland*

MnBi has been restudied by neutron diffraction in order to explain the anomalous magnetic and crystallographic properties of this compound and determine the nature of the observed phase transition at 340–360°C. Below the transition the compound is ferromagnetic with saturation moment  $4.5 \pm 0.2 \mu_B$ . Above the transition the compound is paramagnetic and crystallographically disordered with 15 % Mn-atoms in interstitial positions. On quenching a superstructure appears in which some of the Mn-atoms are in a low spin state. The low moment observed is ascribed partly to this and partly to the presence of antiferromagnetically aligned interstitials.

MnBi has been studied extensively over the last years mainly because of its interesting magnetic properties. However, to a large extent due to the difficulty of preparing pure specimens, conflicting results have appeared, and much of the available information is still uncertain.

At room temperature the compound is ferromagnetic and crystallizes with a hexagonal NiAs-type structure of unit cell dimensions  $a_0 = 4.29 \text{ \AA}$  and  $c_0 = 6.12 \text{ \AA}$ .<sup>1-4</sup> On heating above 360°C there is a first order transition to a paramagnetic<sup>2</sup> or antiferromagnetic<sup>5</sup> state in which the *c*-axis contracts by 3 % and the *a*-axis expands by 1.5 %. A considerable hysteresis seems to be associated with this transition, the ferromagnetic phase appearing again on cooling only below 340°C.<sup>2-4,6</sup>

When quenching from above this transition the change in the unit cell dimensions are frozen in. Guillaud<sup>5</sup> found no moment in the quenched phase, and assumed this and the high temperature phase to be antiferromagnetic. Heikes<sup>2</sup> on the other hand assumed the high temperature phase to be para-

magnetic, and found a linear relationship between  $1/\chi$  and  $T$ . Extrapolating to zero he found a paramagnetic Curie point of 167°C. This was interpreted as the Curie point of the quenched phase, which was found to be ferromagnetic with a saturation moment of  $1.7 \mu_B$ . For the annealed ferromagnetic phase Heikes found a saturation moment of  $3.95 \mu_B$  whereas Guillaud measured  $3.52 \mu_B$ . At 445°C MnBi decomposes to Mn and liquid Bi.

At room temperature MnBi is known to have an extremely high magneto-crystalline energy. This decreases, however, rapidly with decreasing temperature and passes zero around 84°K.<sup>4</sup> One would thus expect the magnetic moment to point along the hexagonal axis at room temperature, and to turn to a direction in the basal plane below 84°K.

Several of the properties mentioned above can best be studied by neutron diffraction, and this method was consequently applied already in 1956 by Roberts.<sup>3</sup> He concluded that the high temperature phase was paramagnetic and crystallographically disordered with 10 % of the Mn-atoms moving into the large trigonal bipyramidal holes of the NiAs structure. He could, however, not exclude an anti-ferromagnetic model in which moments of magnitude  $1.8 \mu_B$  were pointing along the  $c$ -axis, as this also led to fair agreement with the observed intensities. For the quenched phase he assumed the interstitial Mn-atoms to be frozen in, and to disrupt the alignment of the Mn-moments so that only 4/10 of the atoms contributed to the observed moment.

In fitting the room temperature neutron diffraction data on the annealed phase Roberts used a magnetic moment value of  $3.8 \mu_B$  close to that reported by Heikes,<sup>2</sup>  $3.6 \mu_B$ , and thereby derived a rather unusual magnetic form factor for the Mn-ions. Applying the form factor for  $Mn^{2+}$  derived by Shull *et al.*<sup>7</sup> he arrived at a moment value of  $4.3 \mu_B$ . Roberts also took diffraction diagrams at liquid nitrogen and liquid helium temperatures but found only a partial rotation of the moments away from the  $c$ -axis.

The conclusions of Roberts which were based on low intensity and low resolution diagrams obtained on unpure specimens, had to be rather tentative. In view of the important aspects of these conclusions<sup>8</sup> a reinvestigation by neutron diffraction was found of interest.

#### PREPARATION AND EXPERIMENTAL PROCEDURE

The samples were prepared by heating accurately weighed quantities of electrolytical manganese better than 99.9 % pure (British Drug Houses Ltd.) and bismuth 99.98 % pure (Fluka AG) in evacuated quartz tubes. The manganese was crushed and sieved through a  $60 \mu$  sieve before being thoroughly mixed with Bi filings. The mixed powder was pressed to pellets under a pressure of 10 tons/cm<sup>2</sup>. During reaction the temperature was kept between 430° and 440°C for 20–30 days.

It was found of vital importance to keep the temperature within this range. At about 445°C the samples would decompose, and at lower temperatures the reaction would stop at intermediate compositions or proceed only very slowly. It proved impossible to prepare a pure stoichiometric sample as there was always a small amount of unreacted Bi present. As pointed out by Seybolt *et al.*<sup>9</sup> this is probably due to the formation of a layer of stoichiometric MnBi at the surface of the Mn grains, and to the difficulty for Bi or Mn to diffuse through this layer in the absence of concentration gradients.

Most of the samples were cooled down with the furnace to obtain the annealed low temperature phase. However, some samples were quenched rapidly from 400°C. In order



Table 1. Room temperature data on annealed phase.

<i>hkl</i>	$I_{\text{nucl.}}$	$I_{\text{magn.}}$	$I_{\text{total}}$	$I_{\text{obs.}}$ (norm.)	$\Delta$
0001	0	0	0	—	
10 $\bar{1}$ 0	33.67	40.00	73.67	74.36	0.69
10 $\bar{1}$ 1	43.49	0	61.52	61.12	0.40
0002	18.03	0			
10 $\bar{1}$ 2	0.22	7.00	7.22	7.92	0.70
11 $\bar{2}$ 0	4.37	5.69	10.06	10.30	0.24
0003	0	0	0	—	
11 $\bar{2}$ 1	0	0	0	—	
20 $\bar{2}$ 0	8.08	2.78	10.86	12.00	1.14
10 $\bar{1}$ 3	13.40	0	63.31	62.78	0.53
20 $\bar{2}$ 1	13.07	0			
11 $\bar{2}$ 2	34.19	2.65			
20 $\bar{2}$ 2	0.10	1.61	1.71	2.15	0.44
0004	0.72	0	0.72	—	
11 $\bar{2}$ 3	0	0	0	—	
10 $\bar{1}$ 4	9.05	0.17	19.20	18.54	0.66
21 $\bar{3}$ 0	8.88	1.10			
20 $\bar{2}$ 3	7.53	0	22.45	21.70	0.75
21 $\bar{3}$ 1	14.92	0			
21 $\bar{3}$ 2	0.11	0.98	1.09	1.46	0.37
11 $\bar{2}$ 4	2.74	—	4.09	3.82	0.27
30 $\bar{3}$ 0	1.35	—			
0005	0	0	0	—	
30 $\bar{3}$ 1	0	0	0	—	
20 $\bar{2}$ 4	6.08	—	6.08	6.28	0.20
10 $\bar{1}$ 5	5.21	0	29.07	27.89	1.18
21 $\bar{3}$ 3	10.30	0			
30 $\bar{3}$ 2	13.56	—			
2240	0.98	—	0.98	2.07	1.09

$$R = 2.9 \%$$

$c_0 = 6.126 \pm 0.001$  Å. These were determined by a least squares refinement based on the positions of only well resolved reflections.

In Table 1 we compare the calculated nuclear and magnetic intensities with the normalized observed ones. As scattering amplitudes were used  $b_{\text{Mn}} = -0.36 \times 10^{-12}$  and  $b_{\text{Bi}} = 0.86 \times 10^{-12}$  cm. For the atomic positions we have assumed a regular NiAs-type structure, and for the atomic moments a ferromagnetic arrangement with moments of magnitude  $4 \mu_{\text{B}}$  pointing along the *c*-axis. Except for this and the normalizing factor the only parameter introduced was a common isotropic temperature factor,  $\exp(-B(\sin \theta/\lambda)^2)$ , for all atoms. With a value of  $B = 0.7$  Å<sup>2</sup> the discrepancy factor,  $R = \sum |I_{\text{obs}} - I_{\text{calc}}| / \sum I_{\text{obs}}$ , was reduced to 2.9%. In his work Roberts<sup>3</sup> introduced a strongly anisotropic temperature factor implying a soft direction along the *c*-axis. Using his parameters a discrepancy factor of  $R = 3.2$  % was obtained. This difference is insignificant, and as there was no clear evidence that reflections with high *l*-index required a large temperature factor we did not employ an anisotropic temperature factor here.

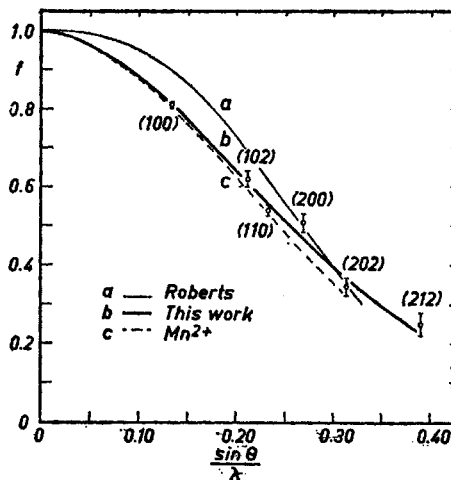


Fig. 2. Experimental form factor values for MnBi compared with the form factor curve for  $\text{Mn}^{2+}$  (c) and form factor curve given by Roberts (a).

The magnetic form factor used was the now well established form factor for the  $\text{Mn}^{2+}$ -ions derived by Hastings *et al.*<sup>10</sup> shown as the dashed curve (c), in Fig. 2. However, at high angles the intensities of the magnetic reflections were systematically higher than calculated and seemed to require a form factor falling off less sharply with  $\sin \theta / \lambda$ . From the observed intensities the form factor values given in Fig. 2 were derived. The vertical bars indicate the probable errors in these values due to the uncertainty in the intensity measurements. The heavy line (b), drawn through the points represents then a better form factor for the Mn-ions in MnBi. The deviation of this curve from that of  $\text{Mn}^{2+}$  at high angles corresponds to a slight contraction of the 3d-shell which is to be expected if the ions are in a  $\text{Mn}^{3+}$ -state. The form factor curve derived by Roberts is shown as curve (a) in Fig. 2. This deviates rather much from the two other curves, evidently due to his attempt to fit the data using the low moment value of Heikes.

Table 2. Data on annealed phase at 5°K.

$hkl$	$I_{\text{nucl.}}$	$I_{\text{magn.}}$	$I_{\text{total}}$	$I_{\text{obs.}}$ (norm.)	$ A $
0001	0	0	0		
10 $\bar{1}$ 0	33.67	24.37	58.04	58.14	0.10
10 $\bar{1}$ 1	43.49	0	43.49	40.48	3.01
0002	18.03	9.04	27.07	25.41	1.66
10 $\bar{1}$ 2	0.22	17.19	17.41	18.69	1.28
11 $\bar{2}$ 0	4.37	3.66	8.03	7.88	0.15
11 $\bar{2}$ 1	0	0	0	0	—
20 $\bar{2}$ 0	8.08	1.83	9.91	11.63	1.72
10 $\bar{1}$ 3	13.40	0	13.40		
20 $\bar{2}$ 1	13.07	0	13.07	64.13	67.18
11 $\bar{2}$ 2	34.19	3.47	37.66		3.05

$$R = 4.8 \%$$

## LOW TEMPERATURE DATA ON ANNEALED PHASE

On cooling to 78°K and 5°K the neutron diffraction diagrams revealed intensity changes characteristic of a turning of the moments from the direction along the *c*-axis to a direction in the basal plane. Only insignificant intensity changes were found between 78°K and 5°K and one can therefore conclude that the turning is practically complete already at 78°K.

The observed intensities at 5°K normalized to the calculated values are given in Table 2. In the calculations we have left out the temperature factor and used the magnetic form factor curve derived above. For the spin quantum number, assuming a spin only moment, we have used  $S = 2.25$  which gave a minimum in the discrepancy factor of  $R = 4.8\%$ . From the effect on  $R$  of changing this value we estimate  $S$  to lie between the limits  $S = 2.25 \pm 0.10$ . The corresponding magnetic moment value  $4.50 \pm 0.20 \mu_B$  is consistent with the moment value  $4 \mu_B$  found at room temperature when assuming a Brillouin type dependence of the moment and a Curie temperature in the vicinity of 360°C. It is strong evidence for the correctness of this value and for the direction of alignment that, with no other parameters involved except for the normalizing factors and the temperature factor at room temperature, discrepancy factors as low as 2.9 and 4.8 % could be obtained. The magnetic moment is larger than that expected for the 4 unpaired electrons of the  $Mn^{3+}$ -ion. However, this can probably be ascribed to an orbital contribution, as Adam and Standley<sup>11</sup> have measured by ferromagnetic resonance technique a  $g$ -value of 2.4 at  $-180^\circ C$ . Thus both the derived form factor curve and the magnetic moment value speaks for a  $Mn^{3+}$  state of the Mn-ions.

## THE HIGH TEMPERATURE PHASE

For the high temperature runs the sample was placed in a vanadium cylinder inside a steel furnace. The furnace was provided with tantalum windows for the neutrons. Separate heating coils above and below the sample, together with thermocouples fixed to the top and the bottom of the sample holder, made it possible to reduce the temperature gradient over the sample to less than 2°.

A neutron diffraction pattern obtained at 390°C is shown in Fig. 3. Except for impurity peaks due to MnO and one Ta-peak due to the furnace, all peaks can be indexed on a hexagonal unit cell of dimensions  $a_0 = 4.38 \text{ \AA}$  and  $c_0 = 6.00 \text{ \AA}$ . These values are in agreement with those of Roberts for this temperature. From the rapid decrease of the observed intensities with diffraction angle the presence of strong thermal vibrations is evident.

In order to decide whether the high temperature phase is paramagnetic or antiferromagnetic we have compared in Table 3 the normalized observed intensities with intensities calculated for a disordered paramagnetic model and an ordered antiferromagnetic model. In each case parameters giving the best possible fit were chosen. For the disordered model this required 15 % interstitial Mn-atoms, and for the antiferromagnetic model effective atomic moments of magnitude  $2.5 \mu_B$  aligned along the *c*-axis. For the temperature factor values of  $B = 3.5 \text{ \AA}^2$  and  $B = 3.0 \text{ \AA}^2$ , respectively, were used.

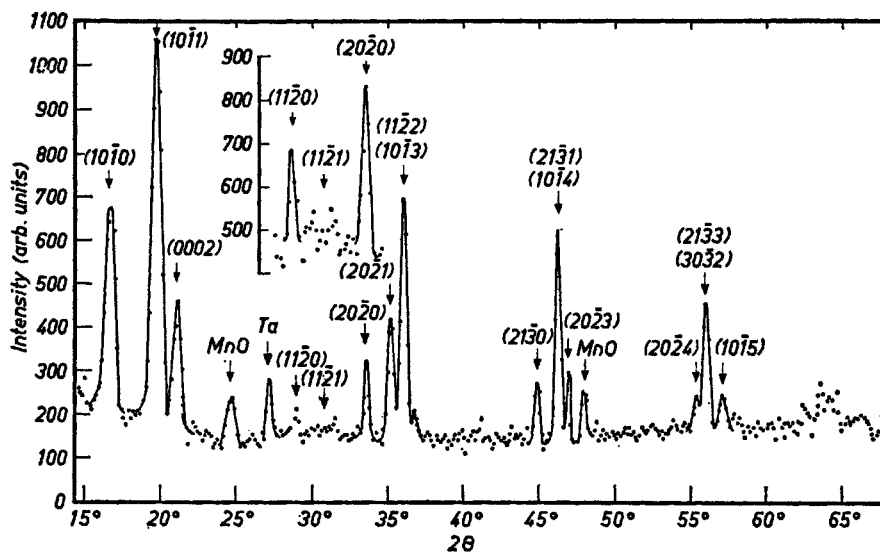


Fig. 3. Neutron diffraction diagram at 390°C,  $\lambda = 1.101 \text{ \AA}$ . Inserted diagram 3 runs added.

Table 3. Data on high temperature phase at 390°C.

$hkl$	$I_{\text{obs.}}$ (norm.)	$I_{\text{calc.}}$ (15 % dis.)	$I_{\text{nucl.}}$ (no dis.)	$I_{\text{magn.}}$ (antiferro)	$I_{\text{total}}$	
10 $\bar{1}$ 0	281.2	275.8	288.8		288.8	
10 $\bar{1}$ 1	472.8	469.6	355.6	118.0	473.6	
0002	132.6	134.3	136.0		136.0	
10 $\bar{1}$ 2	—	3.5	1.5		1.5	
11 $\bar{2}$ 0	30.9	37.3	32.0		32.0	
11 $\bar{2}$ 1	—	0	0	21.1	21.1	
20 $\bar{2}$ 0	51.6	48.8	53.9		53.9	
20 $\bar{2}$ 1	108.9	107.2	84.7	10.0	94.7	
11 $\bar{2}$ 2	303.5	193.2	210.8	2.7	292.2	
10 $\bar{1}$ 3		97.5				78.7
20 $\bar{2}$ 2	—	1.2	0.5		0.5	
0004	—	3.9	3.5		3.5	
11 $\bar{2}$ 3	—	0	0	1.4	1.4	
21 $\bar{3}$ 0	33.3	40.8	47.1		47.1	
21 $\bar{3}$ 1	122.1	91.8	76.3	2.9	122.1	
10 $\bar{1}$ 4		37.0				42.9
20 $\bar{2}$ 3		44.8				37.2
20 $\bar{2}$ 4	23.7	20.0	24.2		24.2	
21 $\bar{3}$ 3	76.4	45.6	39.8	—	93.1	
30 $\bar{3}$ 2		45.2				53.3
10 $\bar{1}$ 5	24.6	24.3	18.7	—	18.7	
		$R = 4.3 \%$			$R = 5.3 \%$	

In both cases very good agreement between the observed and calculated intensities could be obtained, the disorder model leading to a slightly better fit,  $R = 4.3\%$ , than the antiferromagnetic model,  $R = 5.3\%$ . It is hardly possible on the basis of this result to make a decision in favour of one of the two models. However, in calculating  $R$  we have considered only clearly observable reflections. From Table 3 one sees that the next strongest magnetic reflection,  $(11\bar{2}1)$ , which would be purely magnetic, was not observed. This could have disappeared in the background, and to check this possibility further, a part of the diagram was rerun twice. The sum of all three runs is shown as an insert in Fig. 3. In spite of the large scatter in the background points, it is clear that no peak of the expected size appears at the position of the  $(11\bar{2}1)$  reflection.

We therefore assume that the high temperature phase is paramagnetic and disordered with 15% of the Mn-atoms in interstitial positions, but we can not exclude the possibility of an antiferromagnetic phase with a more complicated spin arrangement.

#### THE FIRST ORDER TRANSITION

The transition which takes place between  $340^\circ$  and  $360^\circ\text{C}$  manifests itself in the diffraction pattern through the disappearance of the ferromagnetic reflections and in an abrupt change in the peak positions due to the change in the unit cell dimensions. Both these effects were studied by measuring the intensity and position of the  $(10\bar{1}0)$  reflection as a function of temperature.

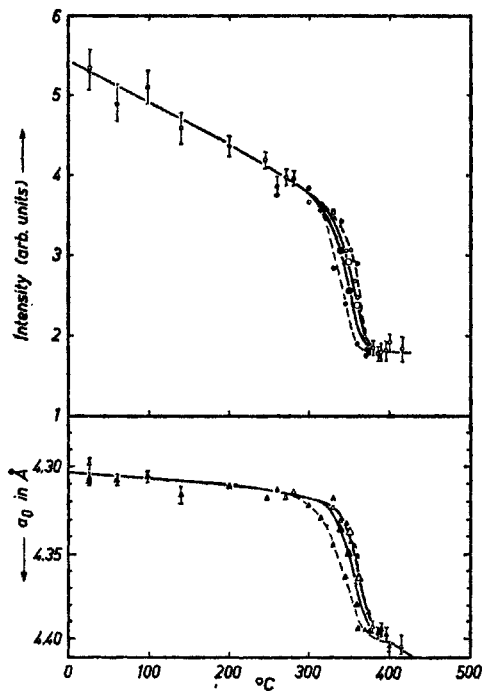


Fig. 4. At the top the integrated intensity of the  $(10\bar{1}0)$  reflection, at the bottom the lattice parameter  $a_0$  as a function of temperature. Open points obtained on heating, closed points on cooling.



In Fig. 4 is plotted at the top the integrated intensity and at the bottom the lattice parameter  $a_0$  as a function of temperature. The lattice parameter was calculated from the peak position which was accurately determined by fitting a Gaussian to the observed points. The vertical bars indicate the estimated standard errors in the measurements. During measurements the temperature was kept constant to within  $\pm 2^\circ$ .

The open points represent values obtained during heating and the closed points during cooling. The first measurements were carried out at approximately 2 hours intervals. Values obtained in this way are represented by the small points in Fig. 3 and exhibit a hysteresis of about  $20^\circ$  as observed by all previous investigators. However, on holding the temperature for a longer period in the transition region a gradual change both in intensity and peak position was observed. Equilibrium condition was only reached after approximately 10 h. Results thus obtained are represented by the large points in the figure. The changes are rather small in the heating cycle, but very pronounced during cooling. To check whether any hysteresis at all remained, we measured for even a longer period of time at the same temperature both on heating and cooling. It proved impossible to obtain the same equilibrium values and it appears that a hysteresis of about  $8^\circ$  still exists.

#### THE QUENCHED PHASE

On quenching through the first order transition the change in the unit cell dimensions could be frozen in, leading to room temperature parameters of  $a_0 = 4.34 \text{ \AA}$  and  $c_0 = 5.97 \text{ \AA}$ . However, a closer inspection of strongly exposed X-ray films (FeK $\alpha$ -radiation) revealed the presence of a number of very weak extra lines, which could only be indexed on a large orthorhombic supercell of dimensions  $a = 11.94 \text{ \AA}$ ,  $b = 8.68 \text{ \AA}$ , and  $c = 7.52 \text{ \AA}$ . This can be derived from the NiAs-type cell by making  $a = 2c_0$ ,  $b = 2a_0$  and  $c = \sqrt{3} a_0$  (see Fig. 5). Since we must assume that the atoms are only slightly displaced from

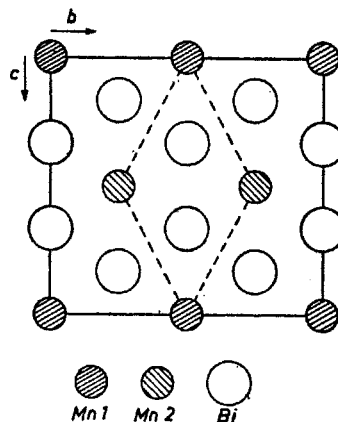


Fig. 5.  $a$ -Axis projection of supercell obtained after quenching, dashed lines indicating NiAs-type cell.

their positions in the NiAs-type structure the symmetry of this cell is not orthorhombic but most likely monoclinic. The only extinction rule which can be derived from the powder data is  $(0k0) = 0$  for  $k = 2n + 1$  so that possible space groups are  $P2_1$  and  $P2_1/m$ . With this low symmetry and 16 Mn-atoms and 16 Bi-atoms per unit cell it seems an impossible task to determine from powder data the direction and magnitude of the atomic displacements.

Also in the neutron diffraction pattern of the quenched phase extra reflections indexable on this large cell becomes visible. A diagram obtained at liquid helium temperature is shown in Fig. 6. Most of the indicated superreflections are weak and to some extent uncertain except for the (001) reflection. This reflection was not observed in the X-ray films, and if purely nuclear, would require large displacements in the  $z$ -direction, which is incompatible with the intensities of the other reflections. We therefore assume (001) to be mainly magnetic in origin, and to arise from a difference in the moments of the Mn1 and Mn2 sites (see Fig. 5). If we assume the magnetic moments to point along the monoclinic  $a$ -axis (hexagonal  $c$ -axis) the observed intensity would require the atoms in one site to have about twice the moment of the atoms on the other. This is possible if the atoms in one site are in a low spin state. Their moments would then be  $2 \mu_B$  instead of  $4 \mu_B$ . With this assumption a reasonable agreement between the observed and calculated intensities for all reflections could be obtained. The only other magnetic superreflection which should be observed is (020) and this is found to be of the correct order of magnitude. A detailed comparison of the observed and calculated intensities is without value as long as the atomic displacements are undetermined.

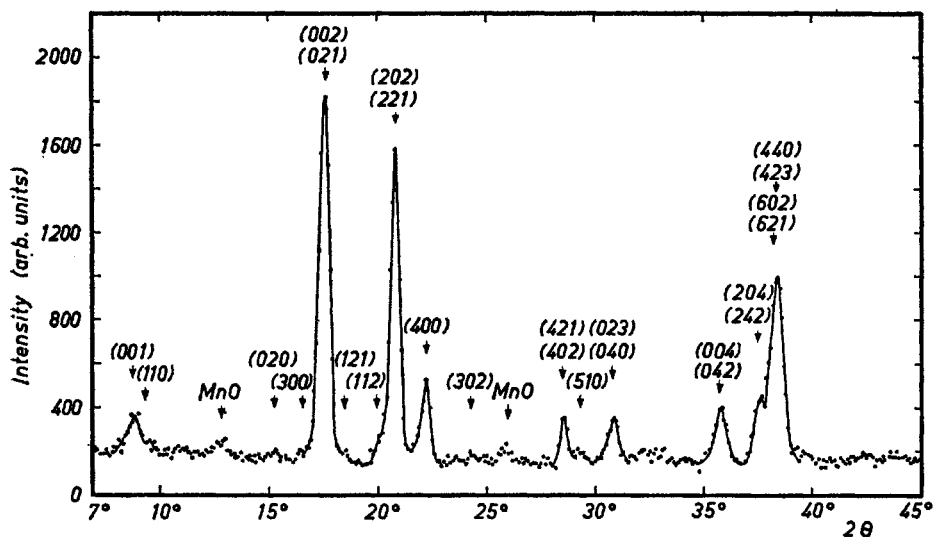


Fig. 6. Neutron diffraction diagram of quenched phase at 5°K,  $\lambda = 1.147 \text{ \AA}$ .

Comparing neutron diffraction diagrams obtained at 5°K, 78°K, and 293°K no significant differences with temperature were observed, except for the intensity decrease due to the thermal motion. Thus there is no sign of a change in the spin direction as observed in the annealed phase.

In the high temperature paramagnetic phase we found 15 % of the Mn-atoms to occupy interstitial sites. After quenching these will most likely remain interstitial, and as near neighbours to the other Mn-atoms will probably through direct exchange interactions orient themselves antiparallel to these. Assuming that half of the other atoms are in a low spin state with moments  $2\mu_B$ , the observed moment per Mn-atom would then be  $(0.85 \times \frac{1}{2}(4 + 2) - 0.15 \times 4)\mu_B = 1.95 \mu_B$ . This is not far from the moment value of  $1.70 \mu_B$  observed by Heikes.

If the quenching were incomplete, the quenched phase would slowly transform to the annealed one even at room temperature. If on the other hand the quenching were about complete, no significant changes could be observed even in the course of several weeks. However, on heating the quenched phase would slowly revert to the annealed one, and at 180°C the transition was complete.

#### DISCUSSIONS AND CONCLUSIONS

The results of this investigation are largely in agreement with those of Roberts, however, with some important modifications. For the low temperature annealed phase both the room temperature and the liquid helium data call for a saturation moment of  $4.5 \pm 0.2 \mu_B$  which is larger than the moment  $3.95 \mu_B$  obtained from magnetization measurements by Heikes,<sup>2</sup> and implied by Roberts. This may be due to the apparently inevitable presence of impurities which will affect the magnetization results but not the neutron diffraction results. Also Roberts stated that his neutron data would lead to a moment value of  $4.3 \mu_B$  if using the  $Mn^{2+}$  form factor of Shull, and it was only by applying a rather unusual form factor that he was able to fit his data with a moment value close to that of Heikes.

Above the 340°–360°C transition the absence of magnetic reflections shows the compound to be paramagnetic, and the observed intensities indicate that 15 % of the Mn-atoms have left their regular lattice sites and occupy the large trigonal bipyramidal holes of the NiAs-structure. This also explains the observed contraction of the *c*-axis.

On quenching from above the transition a superstructure is observed, revealing small atomic displacements. Whether these are also present in the paramagnetic phase we are not able to say, since the intensities of the super-reflections may well be too small for these to become visible in films from the high temperature camera. However, good agreement is obtained for the intensities with calculations based on an NiAs-type unit cell.

In the quenched phase we assume the drastic reduction in the observed moment to result from the presence of the 15 % interstitial atoms, which are most likely antiferromagnetically aligned,<sup>8</sup> and a transition to a low spin state for 50 % of the other Mn-atoms. Goodenough<sup>8</sup> has pointed out that for a Jahn-Teller ion like  $Mn^{3+}$  one might have a transition from a low spin

state at high temperature to a high spin state at low temperature. For MnBi it is possible that the change in the unit cell dimensions on heating above the transition favours a low spin state, but that the distortion observed after quenching leads to a high spin state for some of the ions.

The similarity between MnBi and MnAs is striking. Also in MnAs there is a first order transition from a ferromagnetic to an antiferromagnetic or paramagnetic state, in this case at 40°C. Wilson and Kasper<sup>12</sup> have been able to show that also here the high temperature phase is paramagnetic and the unit cell is distorted from the NiAs-type to the orthorhombic MnP-type. From single crystal X-ray data they were able to determine the atomic displacements which are rather small, and not of the type expected for a Jahn-Teller distortion. Single crystals would also be needed to determine the atomic displacements in MnBi, but the possibilities of making these are rather small, particularly in view of the low decomposition temperature for this compound.

On cooling the annealed phase to 78°K the magnetic moments turned from pointing along the hexagonal *c*-axis to point in a direction in the basal plane. This is in accordance with the observation of Guillaud<sup>4</sup> that the magnetocrystalline energy constant passes zero at 84°K. In the quenched phase no turning of the moment was observed even down to 5°K.

#### REFERENCES

1. Willis, B. T. M. and Rooksby, H. P. *Proc. Phys. Soc. (London)* **B 67** (1954) 290.
2. Heikes, R. R. *Phys. Rev.* **99** (1955) 446.
3. Roberts, B. W. *Phys. Rev.* **104** (1956) 607.
4. Guillaud, C. *Thesis*. University of Strassbourg 1943.
5. Guillaud, C. *J. Phys. Radium* **12** (1951) 143, 223.
6. Himmel, L. and Jack, K. H. *J. Metals* **8** (1956) 1406.
7. Shull, C. G., Strausser, W. A. and Wollan, E. O. *Phys. Rev.* **83** (1951) 333.
8. Goodenough, J. B. *Magnetism and the Chemical Bond*, Interscience, New York 1963.
9. Seybolt, A. U., Hansen, H., Roberts, B. W. and Yurcisin, P. *J. Metals* **8** (1956) 606.
10. Hastings, J. M., Elliott, N. and Corliss, L. M. *Phys. Rev.* **115** (1959) 13.
11. Adam, G. D. and Standley, K. J. *Proc. Phys. Soc. (London)* **A 66** (1953) 823.
12. Wilson, R. H. and Kasper, J. S. *Acta Cryst.* **17** (1964) 95.

Received February 22, 1967.